Numerical Modelling of an Alaska 1964-type Tsunami at the Canadian Coast Guard Base in Victoria, British Columbia

Isaac V. Fine, Richard E. Thomson, Lauren M. Lupton and Stephen Mundschutz

Ocean Sciences Division

Fisheries and Oceans Canada

Institute of Ocean Sciences

9860 West Saanich Road

Sidney, BC

V8L 4B2

2018

Canadian Technical Report of Hydrography and Ocean Sciences 323

Fisheries and Oceans Canada | Pêches et Océans Canada

Canada

Canadian Technical Report of Hydrography and Ocean Sciences

Technical reports contain scientific and technical information of a type that represents a contribution to existing knowledge but which is not normally found in the primary literature. The subject matter is generally related to programs and interests of the Oceans and Science sectors of Fisheries and Oceans Canada.

Technical reports may be cited as full publications. The correct citation appears above the abstract of each report. Each report is abstracted in the data base *Aquatic Sciences and Fisheries Abstracts.*

Technical reports are produced regionally but are numbered nationally. Requests for individual reports will be filled by the issuing establishment listed on the front cover and title page.

Regional and headquarters establishments of Ocean Science and Surveys ceased publication of their various report series as of December 1981. A complete listing of these publications and the last number issued under each title are published in the *Canadian Journal of Fisheries and Aquatic Sciences*, Volume 38: Index to Publications 1981. The current series began with Report Number 1 in January 1982.

Rapport technique canadien sur l'hydrographie et les sciences océaniques

Les rapports techniques contiennent des renseignements scientifiques et techniques qui constituent une contribution aux connaissances actuelles mais que l'on ne trouve pas normalement dans les revues scientifiques. Le sujet est généralement rattaché aux programmes et intérêts des secteurs des Océans et des Sciences de Pêches et Océans Canada.

Les rapports techniques peuvent être cités comme des publications à part entière. Le titre exact figure au-dessus du résumé de chaque rapport. Les rapports techniques sont résumés dans la base de données Résumés des sciences aquatiques et halieutiques.

Les rapports techniques sont produits à l'échelon régional, mais numérotés à l'échelon national. Les demandes de rapports seront satisfaites par l'établissement auteur dont le nom figure sur la couverture et la page de titre.

Les établissements de l'ancien secteur des Sciences et Levés océaniques dans les régions et à l'administration centrale ont cessé de publier leurs diverses séries de rapports en décembre 1981. Vous trouverez dans l'index des publications du volume 38 du Journal canadien des sciences halieutiques et aquatiques, la liste de ces publications ainsi que le dernier numéro paru dans chaque catégorie. La nouvelle série a commencé avec la publication du rapport numéro 1 en janvier 1982.

Canadian Technical Report of
Hydrography and Ocean Sciences 323

2018

NUMERICAL MODELLING OF AN ALASKA 1964-TYPE TSUNAMI AT THE CANADIAN COAST GUARD BASE IN VICTORIA, BRITISH COLUMBIA

by

Isaac V. Fine, Richard E. Thomson, Lauren M. Lupton and Stephen Mundschutz

Ocean Sciences Division
Fisheries and Oceans Canada
Institute of Ocean Sciences
9860 West Saanich Road
Sidney, BC, V8L

© Her Majesty the Queen in Right of Canada, 2018.

Cat. No. Fs97-18/323E-PDF ISBN 978-0-660-25253-7 ISSN 1488-5417

Correct citation for this publication:

Isaac V. Fine, Richard E. Thomson, Lauren M. Lupton and Stephen Mundschutz 2018. Numerical Modelling of an Alaska 1964-type Tsunami at the Canadian Coast Guard Base in Victoria, British Columbia. Can. Tech. Rep. Hydrogr. Ocean Sci. 323: v + 28p.

CONTENTS

1 THE GREAT ALASKA 1964 EARTHQUAKE AND TSUNAMI 1

2 SETUP OF THE NUMERICAL MODEL 3

2.1 Model Setup: Nested Grid Formulation 3

2.1.1 Coarse Grid (Grid 1) 4

2.1.2 Intermediate Grid (Grid 2) 5

2.1.3 Intermediate Grid (Grid 3) 6

2.1.4 Final Grid (Grid 4) 7

2.2 Model Reference Levels 9

2.3 The Source Distribution 9

3 RESULTS 11

3.1 Comparison with the Observed Record at the Victoria Tide Gauge 11

3.2 Maximum Tsunami Wave Heights 12

3.3 Detailed Results for Victoria: Variations of Sea Levels and Tsunami-induced Currents 16

4 CONCLUSIONS 23

5 ACKNOWLEDGEMENTS 25

6 REFERENCES 27

ABSTRACT

Numerical Modelling of an Alaska 1964-type Tsunami at the Canadian Coast Guard Base in Victoria, British Columbia.

Isaac V. Fine, Richard E. Thomson, Lauren M. Lupton and Stephen Mundschutz 2018. Numerical Modelling of an Alaska 1964-type Tsunami at the Canadian Coast Guard Base in Seal Cove, British Columbia. Can. Tech. Rep. Hydrogr. Ocean Sci. 323: v + 28p.

The magnitude 9.2 earthquake that occurred off the coast of Alaska in March 1964 generated large tsunami waves that were responsible for considerable destruction along the west coast of Canada and the United States. The tsunami from the 1964 event is considered a proxy for future tsunamis generated by major Alaska earthquakes. The study is in preparation for upgrades and modernization of the Victoria Coast Guard base.

This work uses a nested-grid numerical tsunami model and an updated three-dimensional viscoelastic model of the 1964 earthquake, combined with a coseismic after-slip model of the rupture zone, to estimate the tsunami waves and currents in Victoria Harbour during the event. The modelled wave heights are found to closely fit the waves recorded by the Victoria tide gauge at the time of the 1964 event.

Modelled tsunami wave amplitudes at the Coast Guard base from a 1964-type event reach 0.56 m above the tidal level and the first wave is the highest. Tsunami-induced currents in the Outer Harbour are strongest where they round Shoal Point, reaching speeds of 0.5 m/s. In the Inner Harbour, current speeds reach 1.5 m/s at the restricted entrance to the Gorge. Incorporation of a 50% safety factor indicates that the safe water level for Victoria should be at least 0.84 m above Mean Higher High Water, or 1.57 m above Mean Sea Level.

RESUME

Modélisation numérique d'un tsunami du type de celui qui a frappé l'Alaska en 1964 à la base de la Garde côtière canadienne de Victoria, Colombie-Britannique.

Isaac V. Fine, Richard E. Thomson, Lauren M. Lupton and Stephen Mundschutz 2018. Numerical Modelling of an Alaska 1964-type Tsunami at the Canadian Coast Guard Base in Victoria, British Columbia. Can. Tech. Rep. Hydrogr. Ocean Sci. 323: v + 28p.

Le tremblement de terre d'une magnitude de 9,2 qui s'est produit au large de l'Alaska en mars 1964 a généré d'importantes ondes de tsunami qui ont entraîné une destruction

massive le long de la côte Ouest du Canada et des États-Unis. Il est considéré comme un indicateur des futurs tsunamis qui seront engendrés par les tremblements de terre majeurs en Alaska. L'étude est effectuée en vue des futures mises à niveau et de la modernisation de la base de la Garde côtière à Victoria.

Ce projet utilise un modèle de tsunami numérique à grille à maille variable et une nouvelle version du modèle viscoélastique tridimensionnel du tremblement de terre de 1964, combinés avec un modèle d'après glissement cosismique de la zone de rupture, pour estimer les ondes de tsunami et les courants dans le port de Victoria pendant un tel phénomène. Les hauteurs de vague modélisées correspondent de près à celles enregistrées par le marégraphe de Victoria pendant le tsunami de 1964.

Les amplitudes des ondes de tsunami modélisées pour la base de la Garde côtière à partir d'un événement du type de celui de 1964 atteignent 0,56 m au-dessus du niveau de la marée et la première vague est la plus haute. Les courants engendrés par le tsunami dans le port extérieur sont les plus forts autour de Shoal Point, où ils atteindront des vitesses de 0,5 m/s. Dans le port intérieur, les vitesses du courant pourraient être de 1,5 m/s à l'entrée restreinte de la Gorge. L'application d'un coefficient de sécurité de 50 % indique que le niveau d'eau sécuritaire de Victoria devrait se trouver au moins à 0,84 m au-dessus de la moyenne des pleines mers supérieures, ou 1,57 m au-dessus du niveau moyen de la mer.

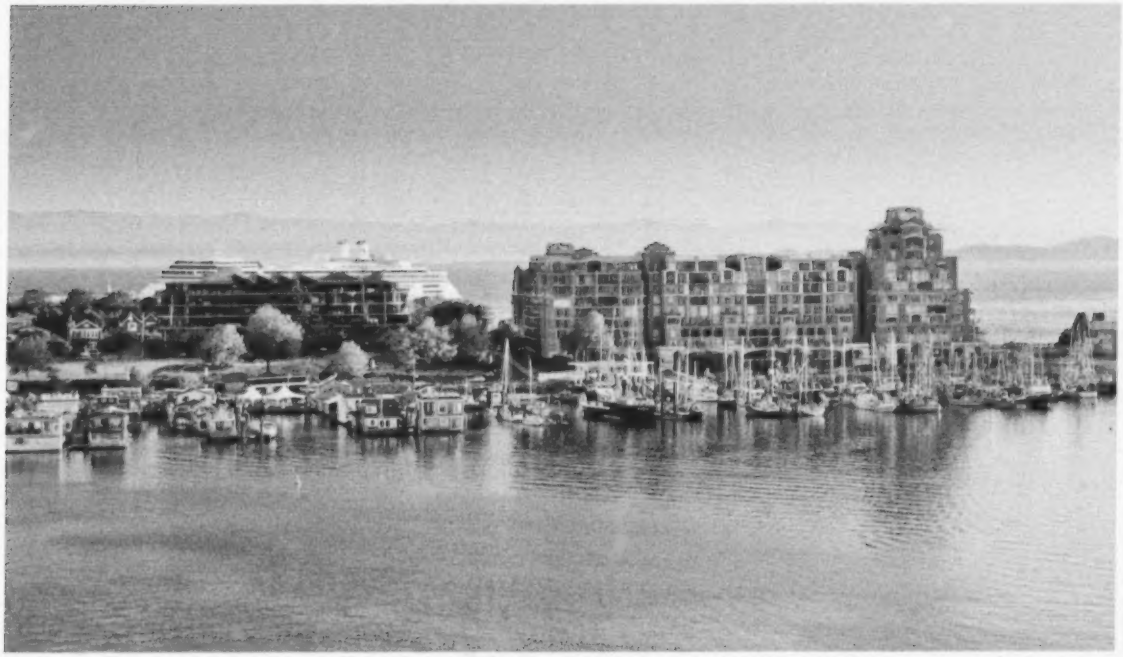

Photo from http://lesleefarrell.com/properties/extraordinary-shoal-point-penthouse

1 THE GREAT ALASKA 1964 EARTHQUAKE AND TSUNAMI

The second strongest instrumentally recorded earthquake in the World Ocean, moment magnitude 9.2 (Mw), occurred off Alaska on March 28, 1964. The event generated a catastrophic tsunami, the second greatest in the 20th century after the 1960 Chilean tsunami, with maximum wave heights of 20 m near the earthquake source region. A large number of landslides and submarine landslides were also initiated, resulting in local tsunami waves as high as 70 m (Lander, 1996). The earthquake, which was the strongest instrumentally recorded earthquake in the North Pacific and second in magnitude only to the Mw=9.5 Chilean earthquake in 1980, occurred in the vicinity of Prince William Sound, leading to the widely used name of the "Prince William Sound Earthquake" (Spaeth and Berkman, 1967). Because of the event date (28 March 1964), the earthquake and associated Pacific-wide tsunami are also called the "Good Friday Earthquake and Tsunami".

The Good Friday tsunami was responsible for close to 130 deaths and about million dollars in damage in Alaska, Washington, California and Hawaii (Spaeth and Berkman, 1967; Lander, 1996; Stephenson et al., 2007). Several locations on the coast of British Columbia suffered major damage (Clague et al., 2003; Anderson and Gow, 2004; Stephenson et al., 2007),

with the highest wave ever recorded in Canada occurring at Shields Bay on the west coast of Graham Island (Haida Gwaii). Here, a wave crest was reported to be 5.2 m above the spring high water, or 9.8 m above tidal datum. Most of the damage from the tsunami occurred in Port Alberni, where a wave reached 4.2 m above the spring-tide high water (Dunbar et al., 1991; Fine et al., 2008).

Several numerical models were constructed to simulate tsunami wave propagation from the 1964 event in the northeast Pacific Ocean (cf. Dunbar et al., 1991; Myers and Baptista, 2001). Although these studies were able to simulate the main features of the tsunami impact on the British Columbia Coast, a more detailed analysis based on recent high-resolution bathymetry and a more refined high-resolution source region of the uplift distribution is needed. Because of its exceptional characteristics, the 1964 Alaska tsunami is typically considered as a proxy for a major future tsunami along the Pacific coast of North America (Suleimani et al., 2013).

The purpose of this report is to simulate the expected tsunami waves for the Canadian Coast Guard base at Victoria Outer harbour, British Columbia, that would be generated by an Alaska 1964-type earthquake with Mw ~ 9.2. This work is part of a larger study to inform future redesigns of Coast Guard stations around the British Columbia coastline to mitigate the impact on the operability of these stations in the event of a major disaster.

2 SETUP OF THE NUMERICAL MODEL

2.1 MODEL SETUP: NESTED GRID FORMULATION

Accurate numerical simulation of tsunami waves in the rapidly shoaling regions of the west coast of British Columbia requires setting up the model domain as a series of nested grids of ever finer spatial and temporal resolution. The use of nested grids of smaller cell dimensions and time steps makes it possible to resolve tsunami wave configurations as they propagate into the shallow coastal regions. The principal requirements for numerical models using nested grids are as follows:

- Nested grid cell sizes are generally obtained by dividing the initial, large-scale coarse numerical grid by an integer, typically 3 to 5. Integers larger than this can lead to grid interface problems;
- Nested grids are needed in near-coastal areas; the coarse "parent" grid should be of sufficient extent to resolve possible feed-back effects that the nested grid may have on the parent grid during the simulation time;
- A good interface between the inner and outer domains is required to avoid errors and model instability associated with point matching between the different grids. This should allow two-way fluxes without trapping shorter waves at the inner domain boundaries;
- High resolution bathymetry, external forcing and observations are needed for model domain setup, initialization and validation at each domain level; here, the nested-grid formulation is similar to that used in well-known tsunami models, TUNAMI and COMCOT (Liu et al., 1998; Imamura et al., 2006; Wang, 2009).

Dispersion effects can be included in the model by substituting numerical dispersion for the actual physical dispersion. Solving this issue (see for example, Imamura et al., 1988) has made it possible for investigators to cover large, open ocean regions, representative of an area affected by a 1964 style tsunami, using a relatively coarse grid with a cell size of roughly 10 km by 10 km (4-5 arc-seconds).

Because of the relatively long periods of the tsunamis generated in the deep water source regions used in this study, and because of the relatively short propagation times of 4 to 5 hours between the source region and Victoria, the dispersion effect is negligible. In this case, high bathymetric resolution is the important factor for modelling wave propagation in the offshore regions.

This project uses a series of four nested grids for the Alaska 1964 tsunami model (Table 1). The choice of model grids takes into account the need for high spatial resolution to accurately resolve the reflection and transformation of the waves and the need for large spatial extent to capture the effects of frequency dispersion during long distance wave propagation.

Table 1: Parameters of the numerical grids used in the tsunami generation and propagation model. Grid extent is along the x (eastward) and y (northward) coordinate directions and is presented in degrees (°). Numerical grid cell sizes for Grids 2, 3 and 4 are roughly 150, 54 and 11 m, respectively. CHS refers to the Canadian Hydrographic Service.

Grid No.	Extent (x, y) (degrees)	Array (number of grid points)	Cell size (x, y; degrees)	Source of data	Processing type
1	34.0, 16.0	4081, 1921	0.00833, 0.00833	GEBCO 30 arc- seconds gridded data	None
2	6.8, 4.235	4085,2542	0.0016667, 0.0016667	BC Coastal Relief, 3 sec; US Coastal Relief, 3sec	Filtering and bilinear interpolation
3	0.22167, 0.21	291, 505	0.0008333, 0.00041667	BC Coastal Relief, 3 sec CHS bathymetry data	Filtering and bilinear interpolation
4	0.12217, 0.0765	740, 920	0.000166667, 0.0000833	CHS bathymetry data	Kriging, smoothing, bilinear interpolation

2.1.1 Coarse Grid (Grid 1)

Grid 1 is the coarsest numerical grid used in the model. This large-scale grid covers the northeast Pacific and encompasses the major source region used in the simulations, the Alaska Fault or failure zone (Figure 2.1). We note that the northeast Pacific is an important tsunami wave generation region through which all offshore tsunamis propagate on their way to the British Columbia coast. The spatial resolution of the grid is 30 arc-seconds in both the east-west direction (spatial scales in the x-direction of 0.45 km to 0.7 km, depending on latitude) and the north-south direction (0.9 km y-direction grid size). The grid is bounded by 45 – 62° N, 157 – 122°

W and was created using the 30 arc-second global bathymetry dataset GEBCO (Becker et al., 2009).

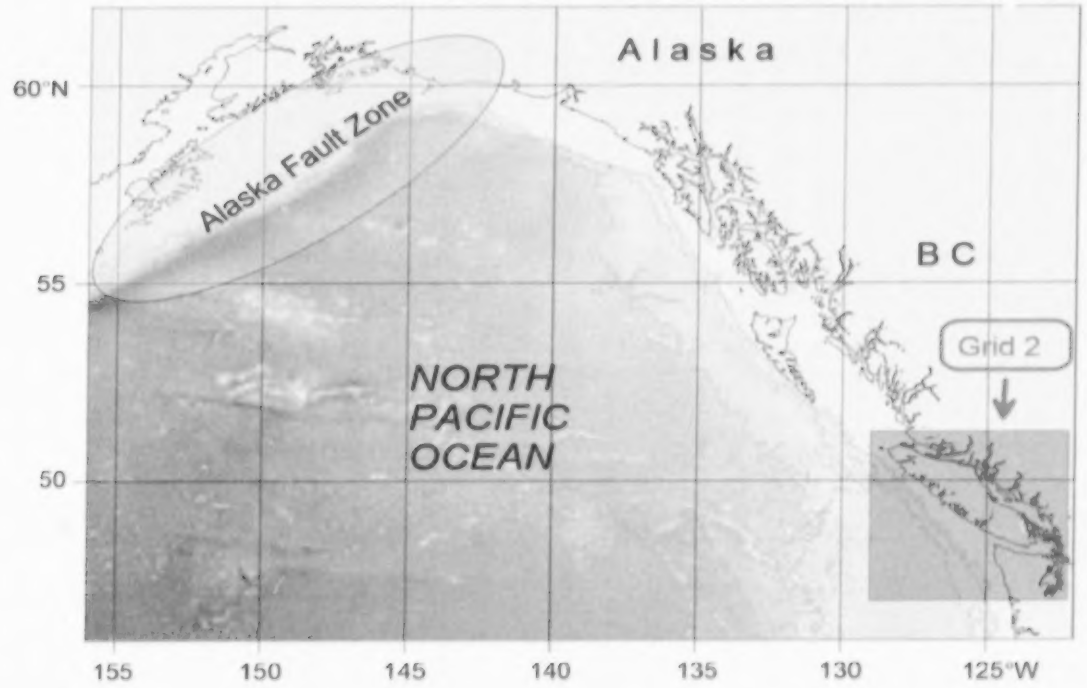

Figure 2.1. The region covered by the large-scale coarse grid numerical model for the northeast Pacific (Grid 1). Also shown is the Alaska Fault Zone that could generate tsunamis that impact the Coast Guard baser. The location of the first nested grid (Grid 2) is shown covering the coast of Vancouver Island.

2.1.2 Intermediate Grid (Grid 2)

Grid 2 covers southern British Columbia and the northwest US Coast (Figure 2.2). The location and coverage of the grid were chosen so that they cover the shelf of Vancouver Island and the surrounding waters. This intermediate grid is important for simulating wave shoaling and wave transformation as the tsunami propagates from the deep ocean to the shelf and into coastal areas. This grid is also important for energy exchange between different parts of the coast and shelf areas.

The northern part of the grid was created using the British Columbia 3 arc-second Digital Elevation Model (NOAA, 2017); the southern part was created using the 3 arc-second US Coastal Relief. Grid 2 has a resolution of 6 arc-seconds in both the east-west direction and in the north-

south direction, corresponding to spatial scales of approximately 125 m and 185 m, respectively (Table 1). The grid spans the northern coast with boundaries of 47 °– 51°N, 129° – 122°W.

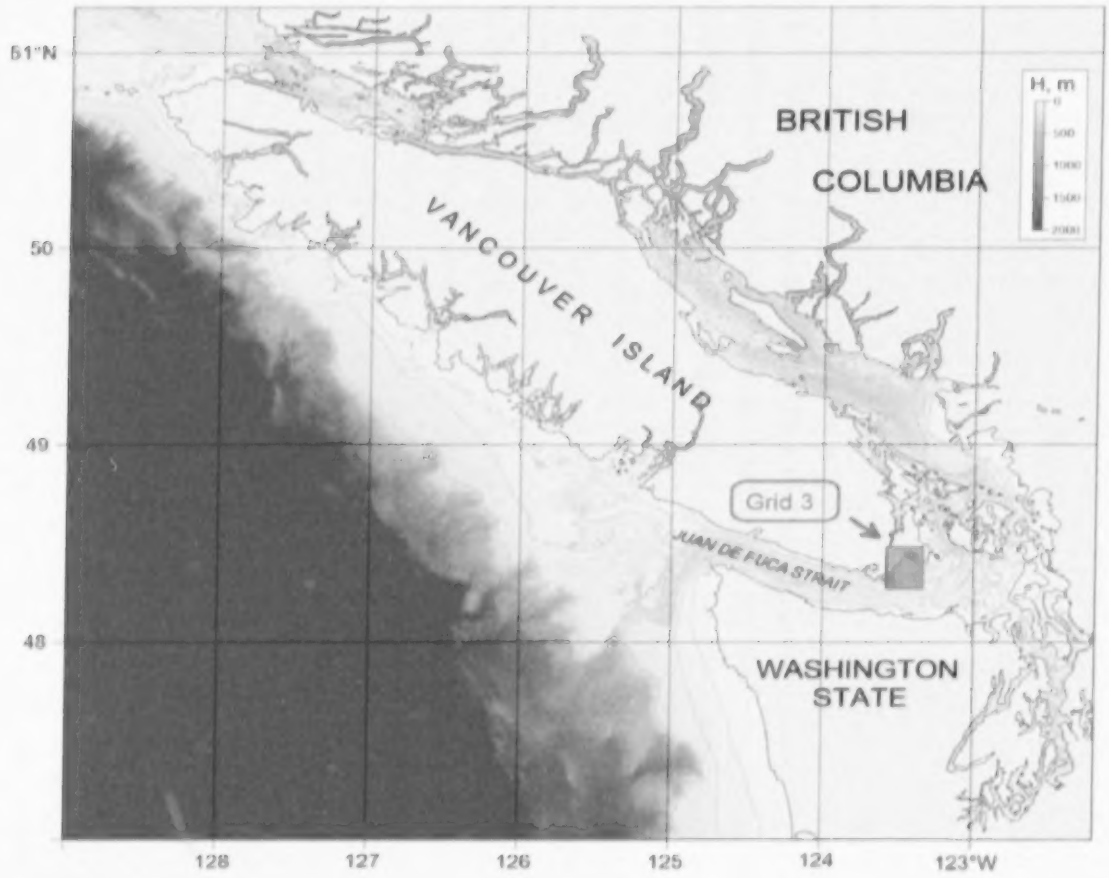

Figure 2.2. The region covered by the medium-scale bathymetric grid (Grid 2) for the Vancouver Island and for the Washington State Coast showing the boundaries and location of the second nested grid (Grid 3) covering the region of Victoria. The horizontal (x, y) grid cell scales for this region are approximately 125 m and 185 m, respectively.

2.1.3 Intermediate Grid (Grid 3)

The third numerical grid covers the southern end of Vancouver Island near Victoria and the surrounding passes and inlets of Juan de Fuca Strait (Figure 2.3). This grid is of considerable importance since it determines the transformation of the incoming waves in the vicinity of Victoria. Model grid cells were created using the British Columbia 3 arc-second bathymetric DEM (British Columbia, 2017). The gridded data were subsequently re-interpolated to a geographical

coordinate system (NAD83 standard) with a rectangular grid-cell size of 3 arc-seconds by 1.5 arc-seconds (approximately 61 m by 46 m) in the east-west and north-south directions, respectively.

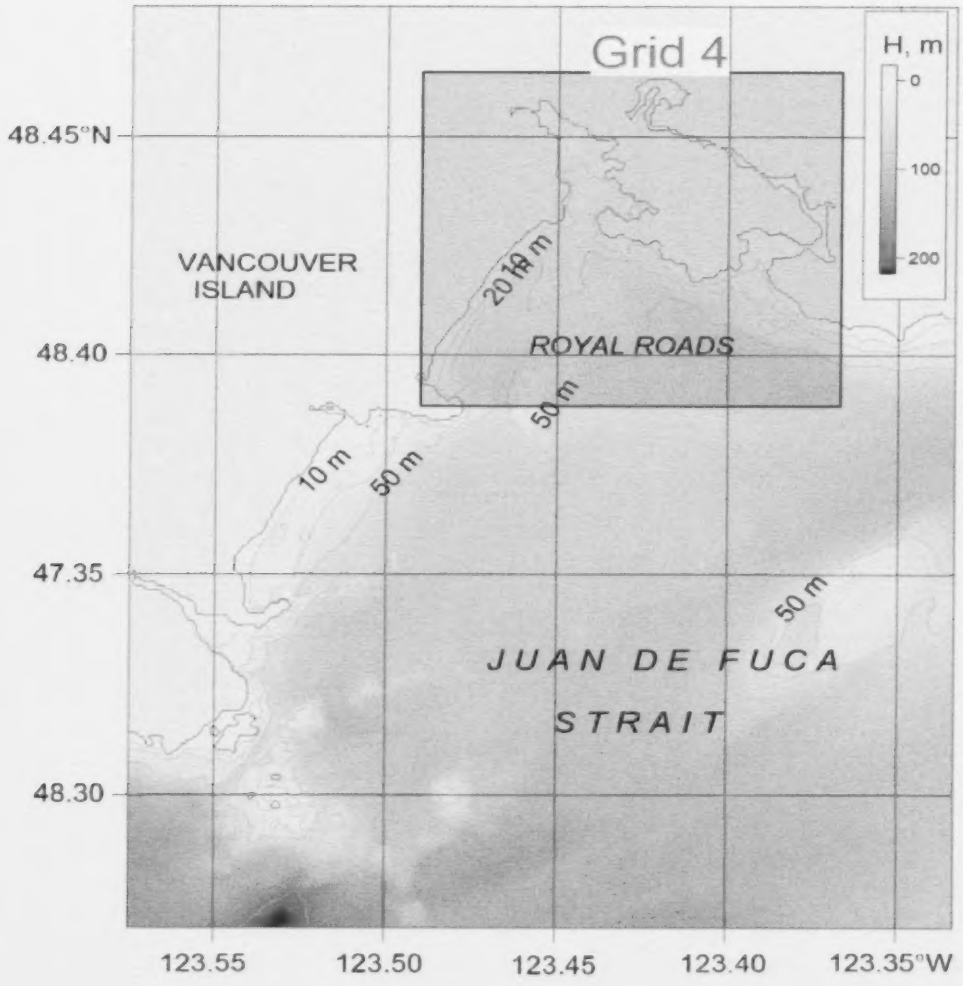

Figure 2.3. Coastal region covered by Grid 3, southern Vancouver Island coast and eastern Juan de Fuca Strait. The grid scale for this region is approximately 61 m by 46 m. The insert shows the boundaries and location of the fourth nested grid (Grid 4) covering Esquimalt Harbour and Victoria Harbour. Depths are in metres (m).

2.1.4 Final Grid (Grid 4)

The final (fourth) numerical grid has the highest spatial resolution and covers coastal areas around Victoria (Figure 2.4). The grid encompasses both Victoria and Esquimalt harbours

and is designed specifically for estimations of tsunami inundation and tsunami-induced currents in the vicinity of the Coast Guard base. A Kriging algorithm (Matheron, 1963) was used to create the grid from the original irregularly spaced bathymetric data. Details on Kriging can be found in Thomson and Emery (2014).

The high resolution grid (x, y) scale is approximately 12 m by 9 m, which enables bathymetric attenuation and amplification effects to be captured. Because the study focuses on a future tsunami, the bathymetry represents the present depths in Victoria Harbour; there have been many changes in the shoreline bathymetry since the 1964 event.

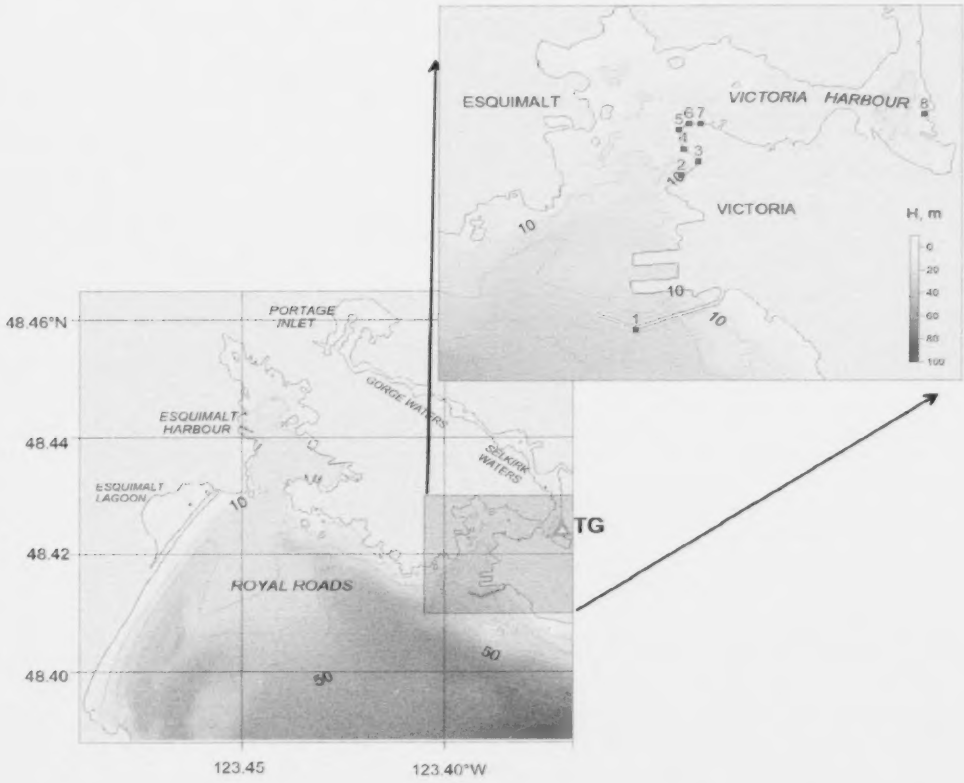

Figure 2.4. The region covered by Grid 4. The fine-scale bathymetric grid has adjusted topography for the region of Victoria Harbour, and has a grid (x, y) scale of approximately 12 m by 9 m. Also shown are the location of the tide gauge (TG) and the sites (1-8) at Victoria for which tsunami wave records have been simulated. Depths are in metres (m).

2.2 MODEL REFERENCE LEVELS

Model simulations are generally conducted for tsunami arrival times that coincide with times of mean higher high water (MHHW), as per recommendations for computation of tsunami inundation in the United States (National Tsunami Hazard Mapping Program, 2010; Nikolsky et al., 2013). Accordingly present values of highest risk, maps of maximum tsunami wave height and current speed presented in this report are referenced to the MHHW mark rather than to the mean tide or to a geodetic reference.

MHHW is used as a reference level for all modelling results. For the Victoria tide gauge, MHHW is 0.73 m above Mean Sea Level (MSL). For convenience, a common reference value of 0.73 m has been applied throughout the region for the tsunami modelling.

Table 2. Chart datum values for station 7120 provided by the Canadian Hydrographic Service. Latitude and longitude are in degrees and minutes. Higher High Water (HHW) is defined in two ways: using all tidal values (Mean) and using only the highest tides (Large). Z_0 is the mean tidal constituent obtained by harmonic analysis of the tidal series.

Tide gauge ID	Name	Latitude (°N)		Longitude (°W)		MSL (m)	HHW (m)		Extreme high water (m)
		Deg	Min	Deg	Min	Z_0	Mean	Large	
7120	Victoria	48	25.48	123	22.42	1.88	2.61	3.12	3.76

2.3 THE SOURCE DISTRIBUTION

Numerical simulation of the 1964 tsunami is based on the newly revised (Suleimani et al., 2013) coseismic slip distribution for the 1964 rupture based on the model of Suito and Freymueller (2009). This is a three-dimensional viscoelastic model, in combination with an after-slip model, which uses realistic geometry with a shallow-dipping elastic slab to describe the post-seismic deformation that followed the 1964 earthquake. The authors applied the inversion-based model by Johnson et al. (1996) as a basis for their coseismic slip model, adjusting it to the new geometry and critically reinterpreting the coseismic data. Suleimani (2011) used results of the near-field modelling of the 1964 tsunami to constrain the amount of slip placed on intraplate splay faults, and to evaluate the extent of the Patton Bay fault. The revised model includes contributions from coseismic horizontal displacements to the initial tsunami wave field from the

component of the ocean surface uplift due to horizontal motion of the steep ocean bottom slopes. The tsunami simulations revealed that including deformation due to horizontal displacements in the source function resulted in an increase in the far-field tsunami amplitudes. The coseismic vertical deformation resulting is shown in Figure 2.5.

Figure 2.5. Seafloor vertical displacements (h (m)) at the source region for the March 1964 Alaska tsunami from Suleimani et al., 2013. Seafloor displacements range from roughly -3 m (blue) to +6 m (red).

3 RESULTS

3.1 COMPARISON WITH THE OBSERVED RECORD AT THE VICTORIA TIDE GAUGE

To verify the model, we compared the modelled results with the record of the Alaska 1964 tsunami at the Victoria tide gauge, in the Inner harbour (Figure 2.4). The original analogue record of the tsunami was first digitized and the tides then carefully subtracted from the digital record using tidal analysis programs (cf. Thomson and Emery, 2014).

Comparisons of the observed and modelled results are shown in Figure 3.1 and Table 3. It is evident that the modelled record fits the observed record quite well. For both the observed and simulated records, the first wave is a crest wave and is the largest wave in the records. The maximum tsunami travel times coincide within 5 minutes, indicating that they are very similar, despite the observations being based on a digitized analogue record.

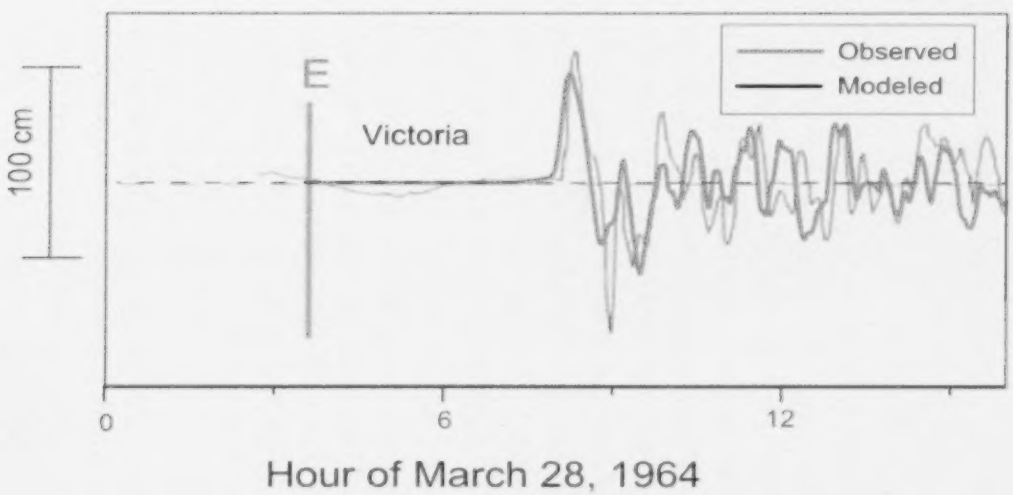

Figure 3.1. Observed versus modelled wave records for the March 1964 Alaska tsunami for the Victoria tide gauge site. The letter "E" denotes the time of the earthquake.

Table 3. Statistical properties of modelled and observed tsunami waves at the Victoria tide gauge location for the March 1964 tsunami source region. Wave heights are in metres and travel times in hours (h) and minutes (min).

	First (maximum) wave			Visible period (min)
	Amplitude (m)	Travel time	Time of maximum elevation (UTC)	
Modelled	0.58	4h 39 min	08:15	40, 90
Observed	0.70	4h 44 min	08:20	40, 90

The maximum wave crest in the modelled record is lower than the maximum of the observed record by 18%. The trailing trough in the modelled wave train is also lower than that in the observed record. However, in general, the shapes of both records are similar and the amplitudes and periods of the ensuing waves are also similar.

The results suggest the model is performing well, with realistic simulations. In part, differences between the observed and modelled records may be related to a change in the harbour shape. Over the more than 50 years between the time of the recorded event in 1964 and the time of the most recent bathymetric data used in the model the harbour has been developed and dredged many times. The model results, which represent the first attempt to model the 1964 tsunami in Victoria Harbour, are based on the modern shape and bathymetry of Victoria Harbour. This approach ensures the model is predicting the effects of future tsunami events and the results are appropriate for risk mitigation applications.

3.2 MAXIMUM TSUNAMI WAVE HEIGHTS

The computed distributions of wave height maxima for a future Alaska-type tsunami based on grids 1-3 are presented in Figures 3.2-3.4. Figure 3.2 shows the "rays" of maximum tsunami wave heights for the entire northeast Pacific. While tsunami wave-height maxima are found in Prince William Sound (the source area), considerable tsunami energy is radiated to the southeast toward the coast of California. In British Columbia and along the US West Coast, the most affected coastal zones are those exposed to the open ocean, such as the west coast of Vancouver Island and the west coast of Washington State. In more protected areas, such as Juan de Fuca Strait, the computed tsunami wave amplitudes are markedly smaller (Figure 3.3; Grid 2).

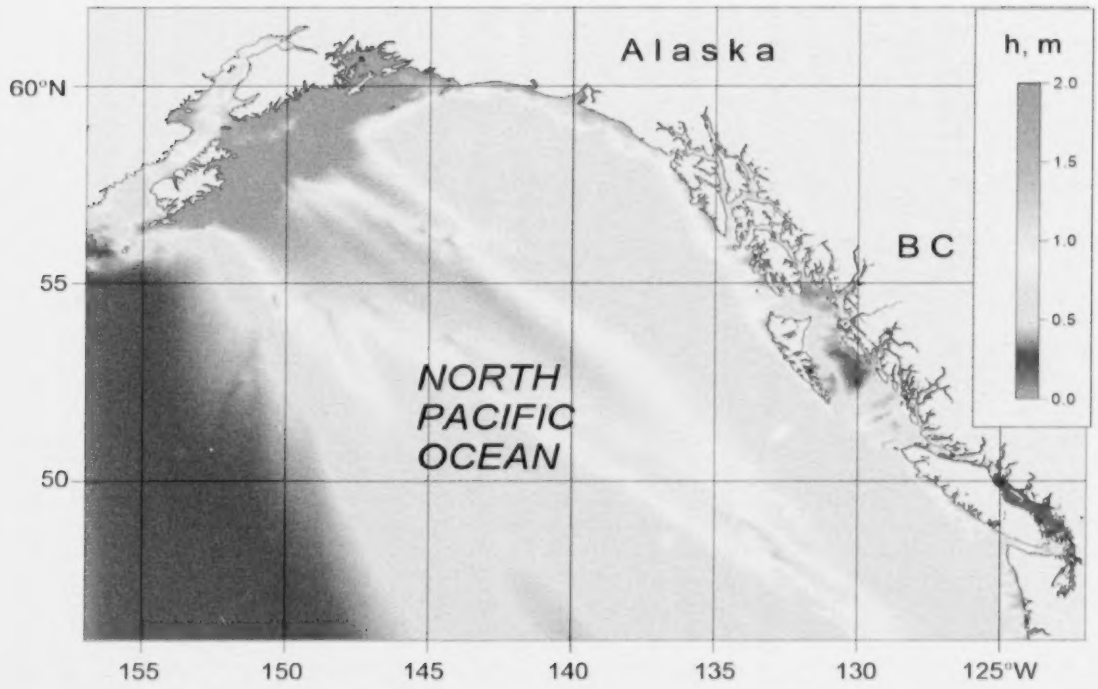

Figure 3.2. Distribution of maximum tsunami wave heights (metres) for Grid 1 of the nested-grid model for waves generated by simulation of the 1964 tsunami.

Results for the finer resolution grids (Grids 3 and 4) demonstrate the considerable spatial variability in the incoming tsunami wave heights for the study region. Figure 3.4 shows the distribution of the tsunami wave heights for Grid 3 in eastern Juan de Fuca Strait off Vancouver Island. As the figure indicates, wave amplitudes increase toward the shoreline and are especially high in Esquimalt Harbour and the upper reaches of Victoria Inner Harbour. Here the wave amplitudes are 3-4 times higher than in the central part of Juan de Fuca Strait. The pronounced increase in tsunami wave heights in the harbours is related to resonance amplification of the incoming tsunami waves.

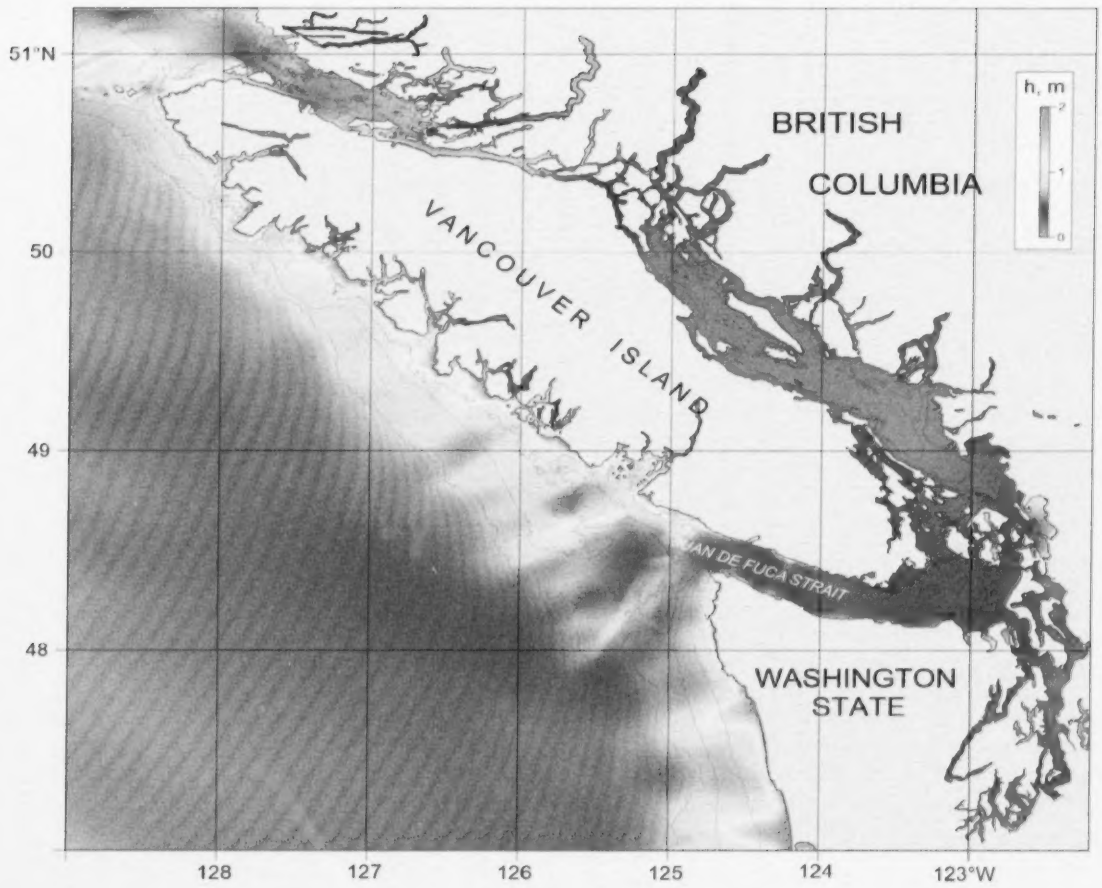

Figure 3.3. Distribution of maximum tsunami wave heights (metres) for Grid 2 of the nested-grid model for waves generated by simulation of the 1964 tsunami.

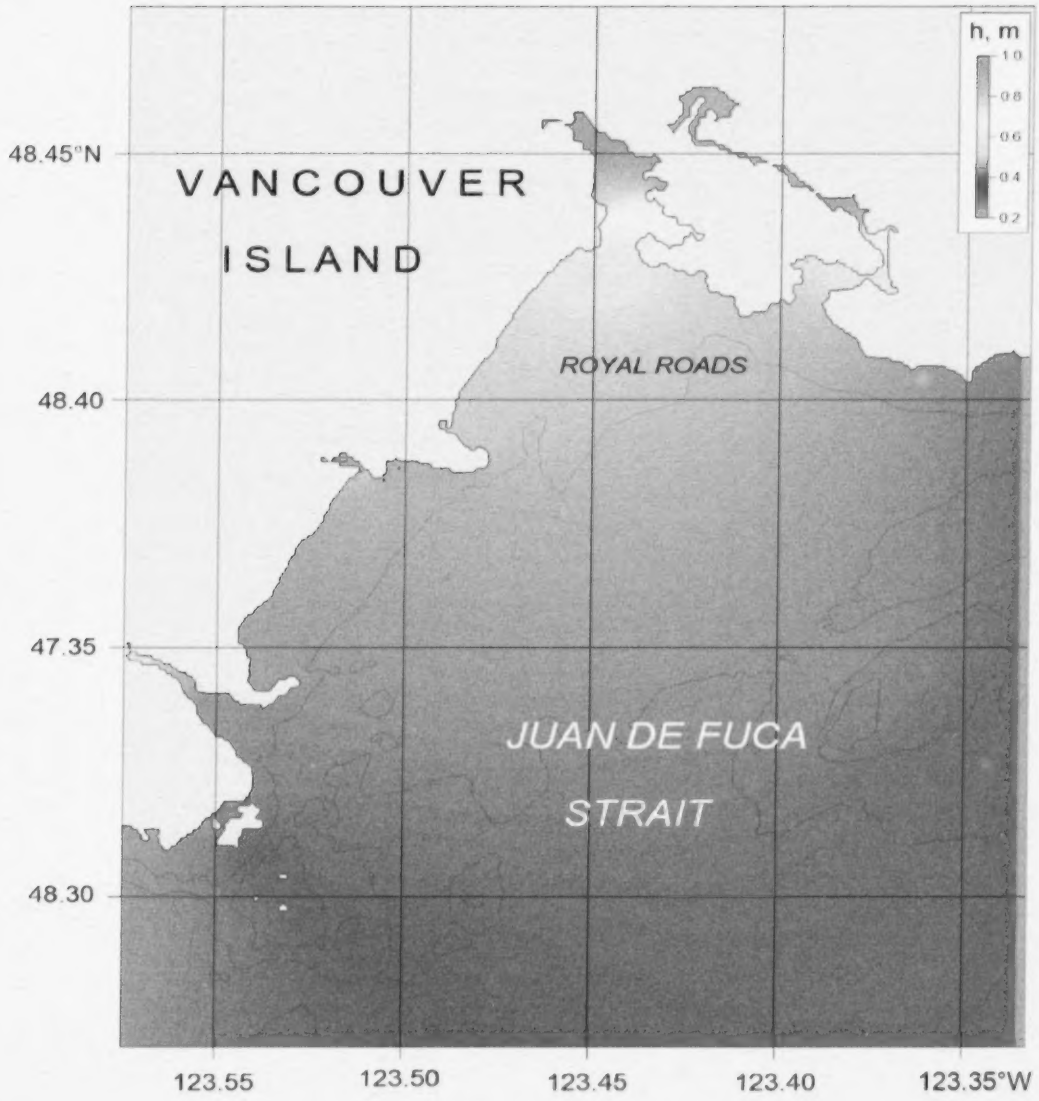

Figure 3.4. Distribution of maximum tsunami wave heights (metres) for Grid 3 of the nested-grid model for waves generated by simulation of the 1964 tsunami.

3.3 DETAILED RESULTS FOR VICTORIA: VARIATIONS OF SEA LEVELS AND TSUNAMI-INDUCED CURRENTS

Figure 3.5 presents a high-resolution map showing the distribution of the maximum tsunami heights in Victoria Harbour and vicinity. We note that the amplitudes of the tsunami waves gradually increase from the entrance to the head of the basin for both Esquimalt Harbour and Victoria Harbour; tsunami heights at the harbour heads (almost 1 m) are up to twice as high as those at the entrance (~0.5 m). At the Victoria Coast Guard base the maximum tsunami wave height is 0.56 m.

Figure 3.6 shows the distribution of the tsunami-induced current maxima derived from the model. Currents near the Coast Guard base are relatively weak and do not exceed 0.5 m/s. In contrast, currents induced in nearby Victoria Inner Harbour exceed 1.5 m/s (3 knots) in mid-stream as the channel narrows on the northern side where it flows into the Gorge. At Site 8, where the tide gauge is located, on the southern side of the Inner Harbour, tsunami-induced currents are noticeably much weaker, with a maximum of 0.2 m/s.

Detailed analysis of the sea level variability and current speeds was carried out for 8 sites around Victoria harbour (Figure 3.5) from the outer breakwater (Site 1) to the location of the tide gauge in the Inner Harbour (Site 8). Figures 3.7 to 3.8 show that the simulated tsunami waves at the Coast Guard base are 5 to10% lower than those at the tide gauge in the Inner Harbour (Figure 3.1).

There is a weak increase in amplitude from Site 1, located at the outer side of the breakwater, to sites 2 to 7, located near the Coast Guard base. However, there is almost no difference in the wave amplitudes at sites 2 to 7 (Figure 3.7) and all records at the Coast Guard base are near identical.

The record at Site 8, corresponding to the tide gauge location, shows 5-10% higher wave heights than at the sites around the Coast Guard base (Figure 3.8). Generally, all records have nearly similar amplitudes, indicating that the spatial extents of the outer and inner parts of Victoria Harbour are short in comparison with the wavelengths of the incoming waves. On the other hand, when the full harbour system is considered (including the shallow Selkirk Waters and Gorge Waters), the incoming waves are significantly amplified.

Records of the wave-generated currents are presented in Figures 3.9 to 3.12. Both current components at Sites 1 to 4 are generally very weak (Figure 3.9-3.10) and typically less than 0.05 m/s. The exception is the eastward component of velocity at Site 1 located at the breakwater, where the current reaches 0.15 m/s. At sites 5 to 7 around Shoal Point, the currents are much stronger than at sites 1 to 4. Especially strong north-south currents of almost 0.5 m/s occur at Site 5 and east-west currents of up to 0.5 m/s occur at Sites 6 and 7. All of these sites

are located on the first peninsula on entering the harbour (Figure 2.4). We further note that the currents are asymmetrical in the positive-negative direction, which may be related to nonlinear effects, and non-uniformly distributed over the study area.

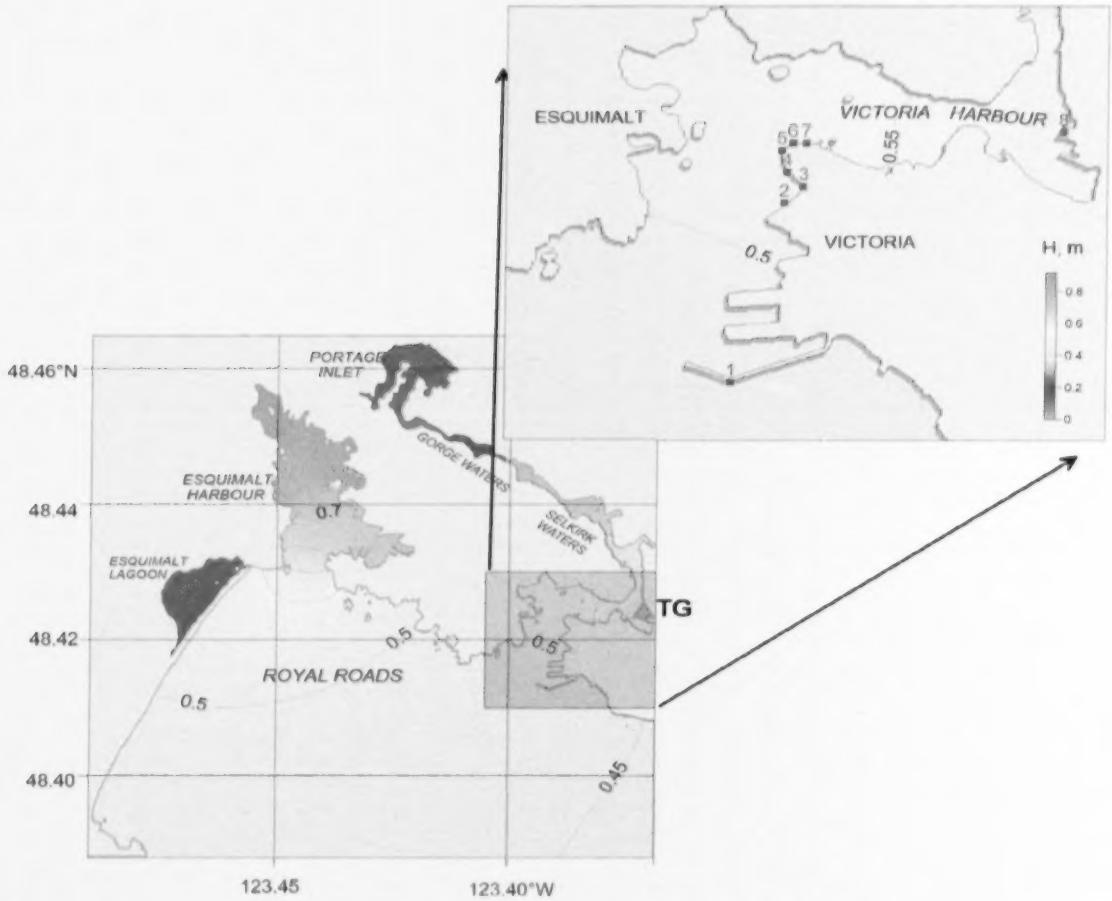

Figure 3.5. Distribution of maximum tsunami wave heights (H in metres) for Grid 4 of the nested-grid model for waves generated by simulation of the 1964 tsunami. Also shown is an enlarged map for Victoria Harbour with the sites 1 to 8 marked.

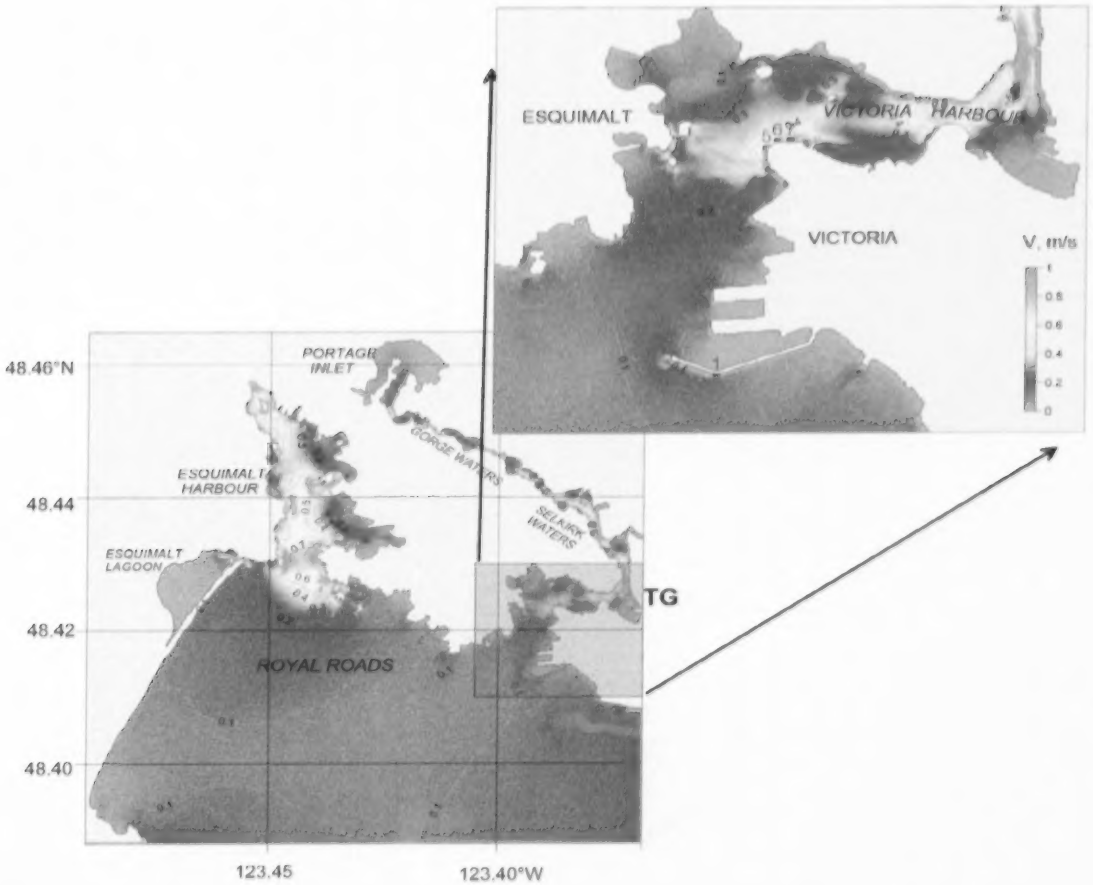

Figure 3.6. Distribution of the maximum tsunami wave-generated currents (V in m/s) for model Grid 4. Also shown is the enlarged map for the Victoria Harbour region.

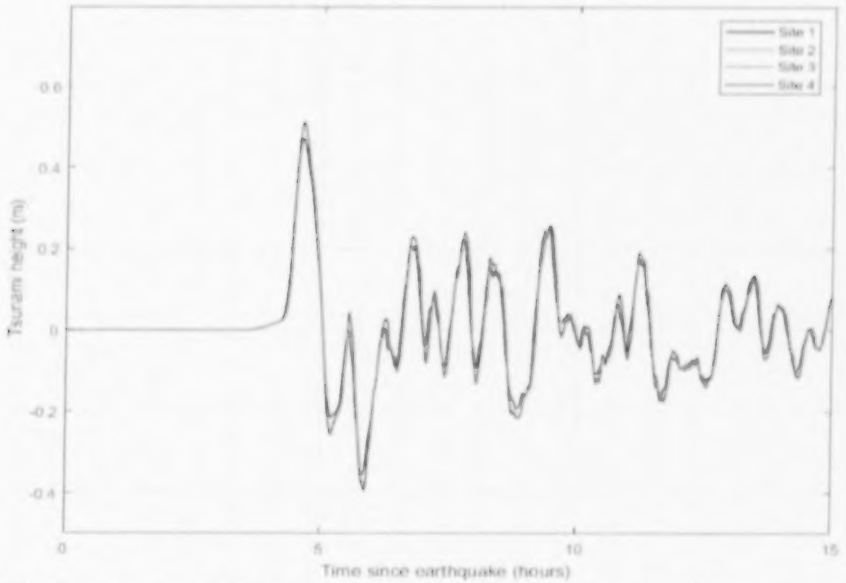

Figure 3.7. Simulated records of sea level variation for the Alaska 1964 tsunami at Sites 1, 2, 3 and 4 (See Figure 3.5 for the site locations).

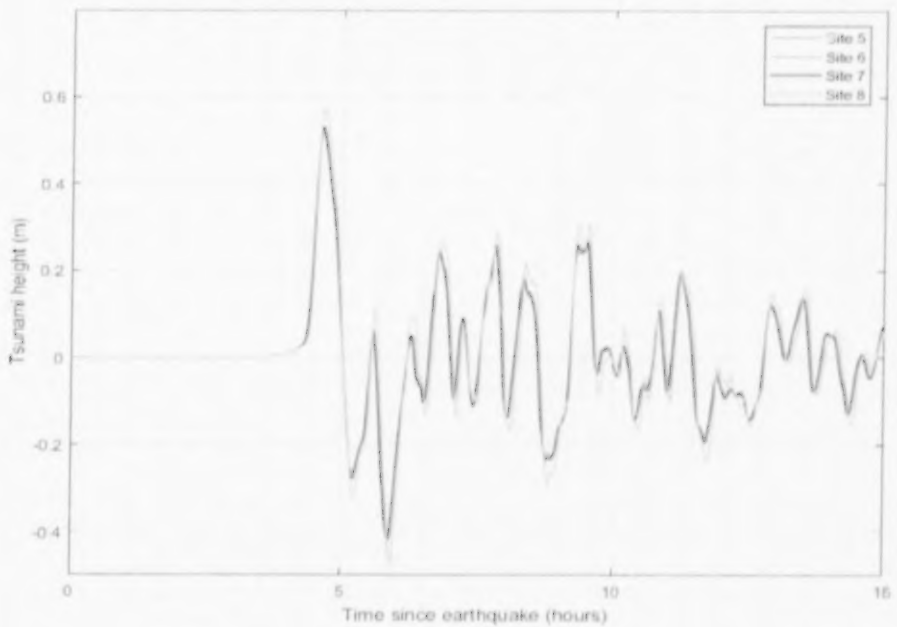

Figure 3.8. Simulated records of sea level variation for the Alaska 1964 tsunami at Sites 5, 6, 7 and 8 (See Figure 3.5 for the site locations).

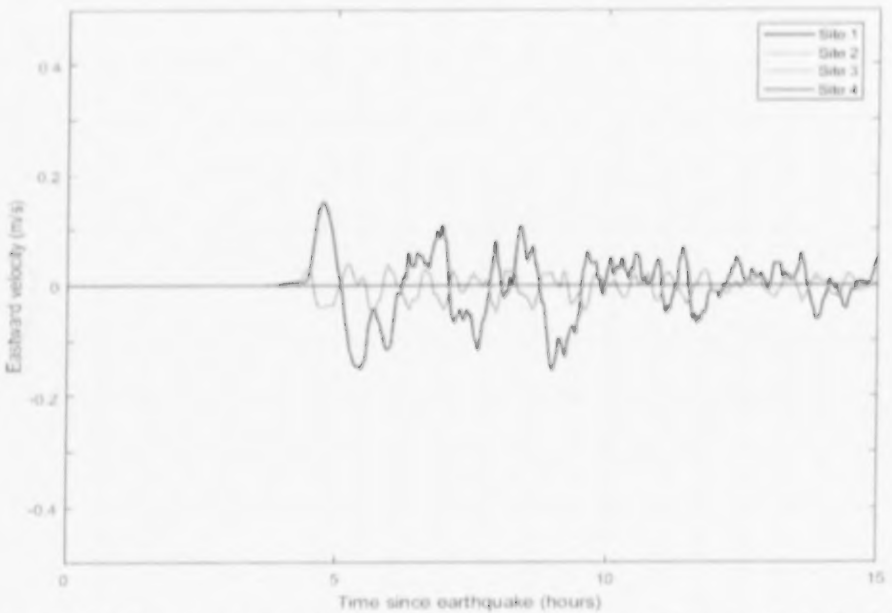

Figure 3.9. Simulated records of the eastward component of current velocity for the Alaska 1964 tsunami at Sites 1, 2, 3 and 4 (See Figure 3.5 for the site locations).

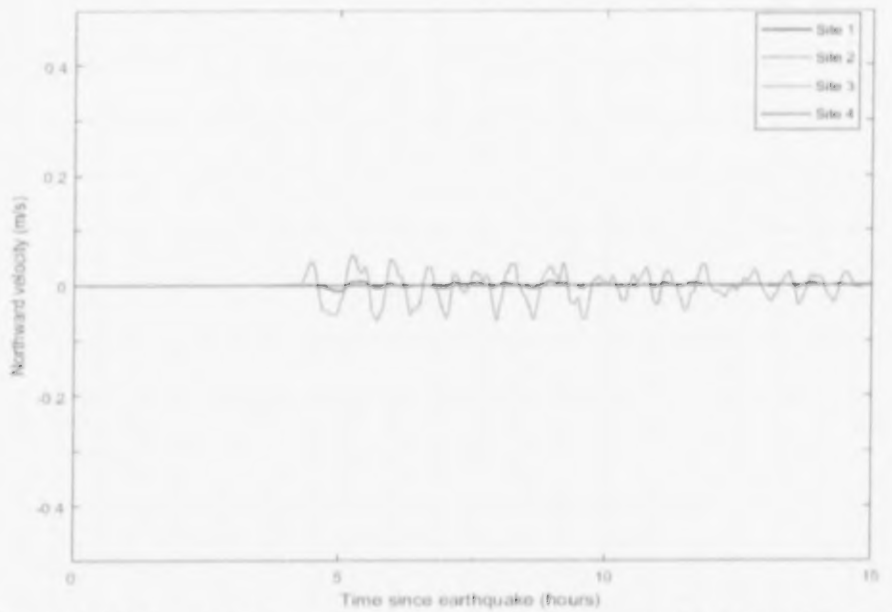

Figure 3.10. Simulated records of the northward component of current velocity for the Alaska 1964 tsunami at Sites 1, 2, 3 and 4 (See Figure 3.5 for the site locations).

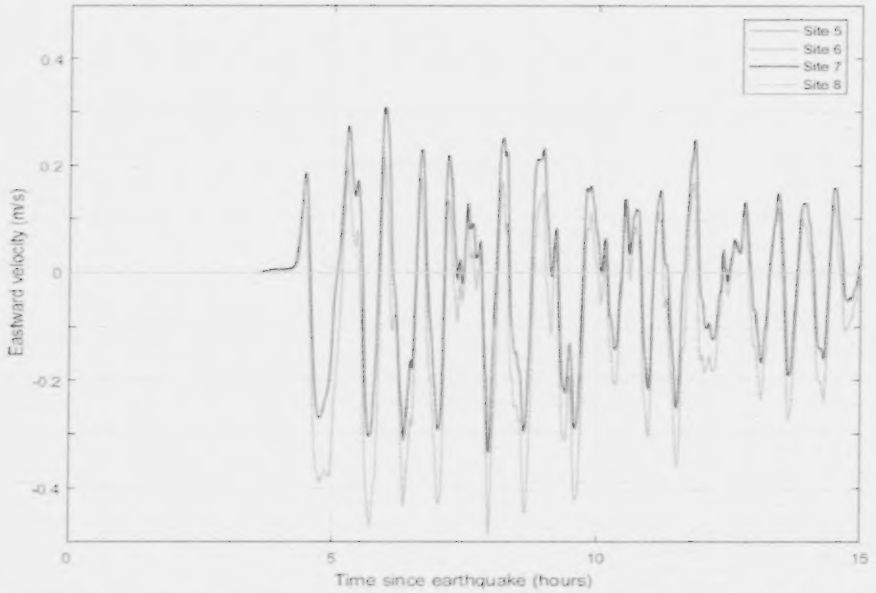

Figure 3.11. Simulated records of the eastward component of current velocity for the Alaska 1964 tsunami at Sites 5, 6, 7 and 8 (See Figure 3.5 for the site locations).

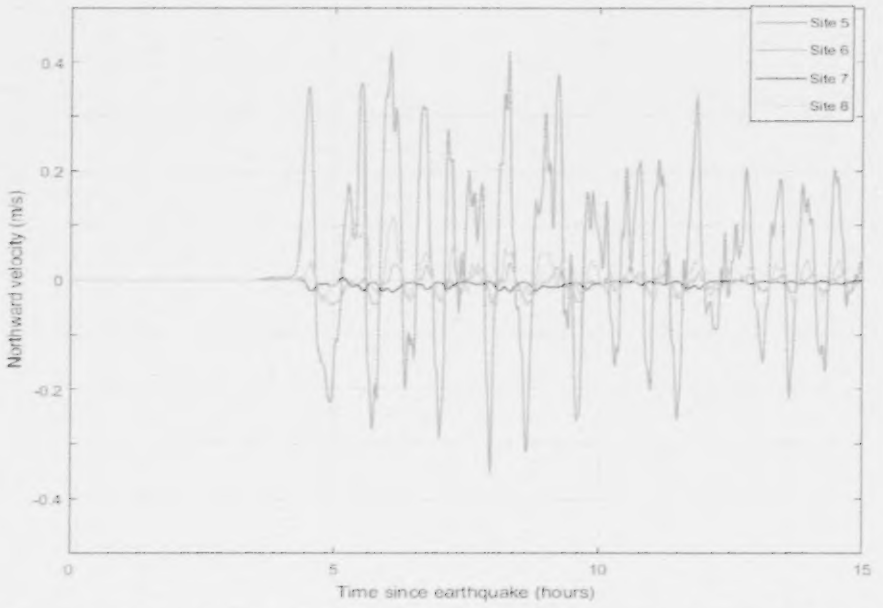

Figure 3.12. Simulated records of the northward component of current velocity for the Alaska 1964 tsunami at Sites 5, 6, 7 and 8 (See Figure 3.5 for the site locations).

This page is left intentionally blank

4 CONCLUSIONS

A high-resolution, nested-grid tsunami model has been used to simulate the distribution of tsunami waves and wave-induced currents that will be generated in Victoria Harbour in the event of an 1964-type Alaska tsunami. The model uses an advanced tsunami source distribution and high-resolution bathymetry for the area of interest. The major results of the modelling are:

- The tsunami at the Victoria Coast Guard base will reach 0.56 m above the tidal level at the time of the wave arrivals, with the first wave being the highest wave;
- The distribution of tsunami wave amplitudes at the Victoria Coast Guard base will be nearly spatially uniform;
- The tsunami will induce moderate currents near the Coast Guard base; currents will be weaker at Sites 2, 3 and 4 and stronger (up to 0.5 m/s) at Sites 5,6,7 located around Shoal Point;
- Currents induced by tsunami waves in the Inner Victoria Harbour will likely reach 1.5 m/s as the northwards flow becomes restricted at the entrance to the Gorge. At the tide gauge (Site 8), the predicted currents will be weak (0.2 m/s or less);

Because details of future possible tsunamis remain unknown in many aspects, we recommend the use of a safety factor of 50%, which should be added to the tsunami amplitudes estimated for a 1964-type event. Based on our analysis of the Alaska 1964 tsunami, the safety level for Victoria should be at least 0.84 m above Mean Higher High Water, or 1.57 m above Mean Sea Level.

This page is left intentionally blank

5 ACKNOWLEDGEMENTS

The authors gratefully thank Peter Wills and Denny Sinnott of the Canadian Hydrographic Service for providing the bathymetric data and tide gauge records for this study, Alexander Rabinovich and Maxim Krassovski of the Institute of Ocean Sciences, for assisting with the data processing and numerical grid formulation, and Elena Suleimani from the University of Alaska at Fairbanks for providing us the latest source model for the Alaska 1964-type earthquake and tsunami. We also thank Alison Scoon for helping transform the original report into a formal technical report.

This page is left intentionally blank

6 REFERENCES

Anderson, P. S. and Gow, G. A. (2004). Tsunamis and Coastal Communities in British Columbia: An Assessment of the B.C. Tsunami Warning System and Related Risk Reduction Practices.75xii pp. (Public Safety and Emergency Preparedness Canada, Ottawa, 2004).

Becker, J. J., D. T. Sandwell, W. H. F. Smith, J. Braud, B. Binder, J. Depner, D. Fabre, J. Factor, S. Ingalls, S-H. Kim, R. Ladner, K. Marks, S. Nelson, A. Pharaoh, R. Trimmer, J. Von Rosenberg, G. Wallace, P. Weatherall. (2009), Global Bathymetry and Elevation Data at 30 Arc Seconds Resolution: SRTM30_PLUS, Marine Geodesy, 32:4, 355-371, DOI: 10.1080/01490410903297766.

British Columbia 3 arc-second Bathymetric Digital Elevation Model (2017). https://www.ngdc.noaa.gov/metaview/page?xml=NOAA/NESDIS/NGDC/MGG/DEM/iso/xml/4956.xml&view=getDataView&header=none.

Clague, J.J., Munro, A., and Murty, T.S. (2003), Tsunami hazard and risk in Canada, Natural Hazards 28 (2-3), 433-461.

Dunbar, D., LeBlond, P., and Murty, T.S. (1991). Evaluation of tsunami amplitudes for the Pacific coast of Canada. Prog. Oceanogr. 26, 115-177.

Fine I.V., Cherniawsky J., Rabinovich A and Stevenson F. (2008). Numerical Modeling and Observations of Tsunami Waves in Alberni Inlet and Barkley Sound, British Columbia. In: Cummins P.R., Satake K., Kong L.S.L. (eds) Tsunami Science Four Years after the 2004 Indian Ocean Tsunami. Pageoph Topical Volumes. Birkhäuser Basel.

Imamura, F., Shuto, N., and Goto, C. (1988). Numerical simulation of the transoceanic propagation of tsunamis. Paper presented at the Sixth Congress of the Asian and Pacific Regional Division. Int. Assoc. Hydraul. Res., Kyoto, Japan. vol.IV, p. 265-272.

Imamura, F., Yalciner, A.C. and Ozyurt, G. (2006). Tsunami modelling manual (TUNAMI model), 2006. http://www.tsunami.civil.tohoku.ac.jp/hokusai3/J/projects/manual-ver-3.1.pdf.

Johnson, J.M., Satake, K., Holdahl, S.R., and Sauber, J. (1996). The 1964 Prince William Sound earthquake— Joint inversion of tsunami waveforms and geodetic data. J. Geophys. Res., 101, no. B1, p. 523–532.

Lander, J.F. (1996). Tsunamis Affecting Alaska, 1737-1996. Boulder, CO: U.S. Department of Commerce.

Liu, P. L.-F., Woo, S-B. and Cho, Y-S. (1998). Computer programs for tsunami propagation and inundation. Technical report, Cornell University.

Matheron, G. (1963). Principles of geostatistics. Economic Geology, 58, pp 1246–1266.

Myers, E.P. & Baptista, A.M. (2001). Analysis of Factors Influencing Simulations of the 1993 Hokkaido Nansei-Oki and 1964 Alaska Tsunamis. Natural Hazards (2001) 23: 1. https://doi.org/10.1023/A:1008150210289.

NOAA (2017). British Columbia 3 arc-second MSL DEM. https://www.ngdc.noaa.gov/dem/squareCellGrid/download/4956. Last access on 11.10.2017.

National Tsunami Hazard Mapping Program (NTHMP) (2010). Guidelines and best practices for tsunami inundation modeling for evacuation planning. NTHMP Mapping & Modeling Subcommittee, NOAA,USA.

Nikolsky, D.J., Suleimani, E.N., Haeusseller, P.J., Ryan, H.F., Kohler, R.D., Combellick, R.A. and Hansen, R.A. (2013). Tsunami Inundation maps of Port Valdez, Alaska. State of Alaska, Department of Natural Resources, Division of Geological & Geophysical Surveys.

Spaeth, M.G., and Berkman, S.C. (1967). The tsunami of March 28, 1964, as recorded at tide stations. Coast and Geod. Survey Techn. Bull. 33, US Department of Commerce, 86 p.

Stephenson, F.E., Rabinovich, A.B., Solovieva, O.N., Kulikov, E.A. and Yakovenko, O.I. (2007). Catalogue of tsunamis, British Columbia, Canada: 1700-2007. Preprint. P.P. Shirshov Inst. Oceanology, Moscow, 134 p.

Suito, H., and Freymueller, J.T. (2009). A viscoelastic and after-slip post seismic model for the 1964 Alaska earthquake. J. Geophys. Res., 114, B11404, doi: 10.1029/2008JB005954.

Suleimani, E.N. (2011). Numerical studies of tectonic and landslide-generated tsunamis caused by the 1964 Great Alaska Earthquake. Fairbanks, Alaska, University of Alaska Fairbanks, Ph.D. dissertation, 181 p.

Suleimani, E.N., Nicolsky, D.J., and Koehler, R.D. (2013). Tsunami Inundation Maps of Sitka, Alaska. Report of Investigations 2013-3, State of Alaska, Department of Natural Resources, Division of Geological and Geophysical Surveys, Fairbanks, AK, 76 p., 1 sheet, scale 1:250,000. doi: 10.14509/26671.

Thomson, R.E. and Emery, W.J. (2014). Data Analysis Methods in Physical Oceanography: 3rd Edition. Elsevier Science, Amsterdam, London, New York (August 2014), 716 p.

Wang, X. (2009). User Manual for COMCOT Version 1.7. http://ceeserver.cee.cornell.edu/pll-group/doc/COMCOT_User_Manual_v1_7.pdf.